Cellulose (2019) 26:569–580
https://doi.org/10.1007/s10570-018-2101-z

ORIGINAL PAPER

TEMPO-oxidized cellulose nanofiber-reinforced lignin based polyester films as a separator for electric double-layer capacitor

Shogo Taira · Makoto Kurihara · Keiichi Koda · Kazuki Sugimura · Yoshiyuki Nishio · Yasumitsu Uraki

Received: 30 August 2018 / Accepted: 2 November 2018 / Published online: 13 November 2018

Abstract Recently we developed a self-standing and flexible lignin-based polyester film (LPF) as a separator for electric double-layer capacitor (EDLC). However, the film showed very low mechanical strength. In this study, reinforcement of LPF was attempted with TEMPO-oxidized cellulose nanofiber (TOCN). Modulus of elasticity was remarkably increased with an increase in TOCN content. By 1% addition of TOCN, tensile strength at failure was also significantly increased with its flexibility maintained, resulting in the highest strain energy density among tested samples. Zero-span tensile test revealed that the improved tensile strength was caused by the TOCN strength. In addition, dynamic mechanical analysis and differential scanning calorimetry demonstrated that TOCN suppressed thermal deformation of LPF at elevated temperature. However, TOCN did not affect the tensile impact strength of the LPF. Finally, EDLC was assembled with the TOCN-reinforced LPF as a separator, hand-made electrodes with commercial activated carbon and conductive carbon black, and triethylmethylammonium tetrafluoroborate/propylene carbonate as an organic electrolyte. Although this EDLC showed higher specific capacitance than EDLC with commercial cellulosic separator as a reference, intrinsic and charge transfer resistances of this EDLC were much higher than those of the reference EDLC. By conversion of the LPF to porous film, the resistances were dramatically improved, and the specific capacitance was further enhanced. Consequently, LPF reinforced with 1% TOCN is a promising separator for EDLC.

Electronic supplementary material The online version of this article (https://doi.org/10.1007/s10570-018-2101-z) contains supplementary material, which is available to authorized users.

S. Taira
Graduate School of Agriculture, Hokkaido University, Sapporo 060-8589, Japan

M. Kurihara
Graduate School of Environmental Science, Hokkaido University, Sapporo 060-0810, Japan

K. Koda · Y. Uraki (✉)
Research Faculty of Agriculture, Hokkaido University, Sapporo 060-8589, Japan
e-mail: uraki@for.agr.hokudai.ac.jp

K. Sugimura · Y. Nishio
Graduate School of Agriculture, Kyoto University, Kyoto 606-8502, Japan

Graphical abstract

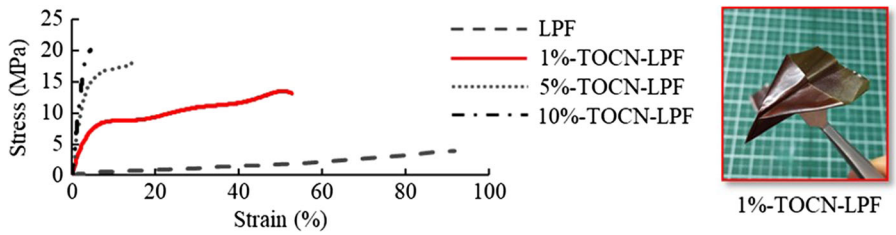

Keywords TEMPO-oxidized cellulose nanofiber · Lignin-based polyester film · Electric double-layer capacitor · Self-standing polymeric film

Introduction

In wood components, cellulose and its derivatives are widely used in our daily life and cover wide applications in the many industrial fields (He and Zhao 2007; Li et al. 2007; Lee et al. 2014; Sugimura et al. 2015). However, lignin utilization is limited despite its natural abundance next to cellulose (Calvo-Flores and Dobado 2010; Wu et al. 2017; Nihat and Nilgül 2002). As an aim of lignin utilization, we have developed lignin-based polyester films, and reported its application as separator material for electric double-layer capacitor (EDLC) (Kubota et al. 2015). EDLC with large power density is expected to be one of the promising electric energy storage devices in the next generation (Choi et al. 2012; Gogotsi and Simon 2011; Sharma and Bhatti 2010). EDLC consists basically of polarizable electrodes, separator, electrolyte and current collector, in which the former two components are manufactured from organic polymer materials. We have also reported to fabricate electrode material from several types of technical lignin (You et al. 2015, 2016a, b). Therefore, if high-performance separator is successfully prepared from lignin, then it means all organic polymer parts in EDLC can be substituted with lignin-based material. Required properties for separator material include electrical insulation for a pair of electrode, electrolyte permeability, chemical stability and toughness with flexibility (Arora and Zhang 2004). So far, cellulose and synthetic polymers, such as polyethylene and polypropylene, have been used commercially as a material to fulfill such requirements for separator material (Szubzda et al. 2014; Tõnurist et al. 2012; Noorden et al. 2014).

A lignin-based polyester film (LPF) as a candidate of separator material was firstly attempted to be prepared by melt-polycondensation reaction of binary components, polyethylene glycol-lignin (PEG-L) as an organosolv lignin (Lin et al. 2012; Gillet et al. 2017; Koumba-Yoya and Stevanovic 2017) and maleic anhydride (MA), where PEG-L and MA were used as polyol component and dicarboxylic acid anhydride, respectively. The reason why PEG-L was used as a raw material was its high reactivity and thermal fusibility, which would accelerate melt-polycondensation reaction for film preparation. Hydroxy groups of PEG moiety introduced into the lignin skeleton was considered more accessible to MA than original hydroxy groups in lignin skeleton, and flexibility of PEG moiety gave lignin high thermal mobility (Lin et al. 2012). Unexpectedly, the film was found not to act as a separator. The reason was assumed to be the lack of flexibility. To add flexibility to the film, polyethylene glycol with a molar mass of 500 kDa (PEG500k) as a flexible polymer was blended with above binary components (Kubota et al. 2015). The resultant film of these ternary components showed a slightly improved separator performance compared to the film of the binary components. The performance was further improved by conversion of the film into porous one. However, this film still had a drawback; very low tensile strength. In this study, the reinforcement of tensile strength was attempted by the addition of cellulose nanofiber (CNF) as a filler (Yano et al. 2005).

Some types of CNF have been proposed as a filler material (Isogai et al. 2011; Kose et al. 2011; Kaitsuka et al. 2016). Among them, we focused on TEMPO-oxidized cellulose nanofiber (TOCN) because TOCN is well dispersed in water and commercially available (Okita et al. 2010; Saito et al. 2009). In this article,

main objectives are to prepare LPF comprised of quaternary components including TOCN of different charge amounts, and to clarify the effect of TOCN on mechanical properties of the resultant TOCN-containing LPF (TOCN-LPF), such as tensile strength and viscoelastic properties. In addition, the EDLC was assembled with the resultant film as a separator, and its electrochemical properties were evaluated. Finally, an improvement of its electrochemical properties was attempted by the conversion of the film to more porous film by the addition of NaCl powder to the quaternary components before melt-polycondensation and the removal of the NaCl powder after melt-polycondensation.

Experimental

Preparation of ternary LPF

Ternary LPF was prepared, according to our previous study (Kubota et al. 2015). Briefly, 1.2 g of PEG with a molar mass of 500 kDa (PEG500k) and 1.66 g of polyethylene glycol-lignin (PEG-L) were dissolved in chloroform with vigorous stirring to yield a homogeneous solution. PEG-L was kindly supplied from Harima Chemicals Group, Inc. (Tokyo, Japan), which was prepared from Japanese cedar chips by organosolv pulping with PEG400 and sulfuric acid (Lin et al. 2012). After the solvent evaporation, the mixture (0.145 g) was mixed with MA (0.058 g) by using a mortar and a pestle in a glove box under a nitrogen atmosphere. Here, a Teflon sheet (50 μm in thickness) was placed on a hot-pressing machine and a self-made Teflon spacer as a mold (5 cm × 5 cm in a rectangular shape, 50 μm in thickness) was put on the sheet. The mixture of ternary components (0.15 g), PEG-L, PEG500kDa and MA, was set in the Teflon spacer and covered with another Teflon sheet. The sheets were pressed to allow melt-polycondensation reaction of the mixture to proceed under 5 MPa at 200 °C for 4 h, where heating-up time to 200 °C was about 1 h. After cooling to 30 °C for about 1 h, the fabricated LPF was taken out of the Teflon sheets and the spacer.

Preparation of TOCN-LPF (PEGL/MA/PEG500k/TOCN)

Four, twelve, twenty and forty grams of TOCN aqueous suspension (1% consistency), which was supplied from Nippon Paper Industry (Tokyo, Japan), was separately diluted with 50 mL water and stirred for 1 h. PEG500k (1.2 g) was suspended in each diluted TOCN suspension with stirring overnight. PEG-L (1.66 g) was added to the mixed suspension, and the resulting mixture was further stirred overnight, and lyophilized. The freeze-dried mixture (0.145 g) was separately blended with MA (0.057, 0.055, 0.054 and 0.051 g) by using a mortar and a pestle. As a result, TOCN contents in the mixture were 1, 3, 5 and 10%, respectively, based on the ternary component of PEG-L/MA/PEG500k. PEG-L/MA/PEG500k ratio in the resultant quaternary mixture was fixed at 41.5/28.5/30. The resultant quaternary mixture was hot-pressed under the same conditions as mentioned above to obtain TOCN-LPF.

Preparation of porous TOCN-LPF

NaCl granules were crushed with a Wonder Blender WB-1 (OSAKA CHEMICAL Co.,Ltd., Osaka, Japan) for 2 h, and dried overnight in vacuo at 50 °C. NaCl powder with less than 300 μm in diameter was collected with stainless sieves. 40 mg of powder was added to the quaternary mixture and mixed well with a mortar and a pestle. The NaCl-containing mixture was hot-pressed under the above conditions to obtain a film. The film was washed with distilled water by shaking at r.t. for 2 days.

Characterization of obtained films

Transmission and attenuated total reflection (ATR) Fourier transform infrared (FTIR) spectra were measured on a JASCO FT/IR-4100 spectrophotometer (Tokyo, Japan). For transmission measurement, KBr pellets of specimens were prepared by mixing approximately 1 mg of samples and 200 mg of KBr. For ATR measurement with single reflection, a film was placed on a sample chamber in an ATR device (JASCO ATR PRO450-S, Tokyo, Japan).

Contact angles were measured on a Dropmaster300 (Kyowa Interface Science Co., Ltd., Saitama, Japan) by dropping 5 μL of deionized water to specimen at

room temperature. A photo of the droplet on the specimen was taken at 0 s, 30 s, 1 min and 5 min after dropping. A contact angle was calculated from the photo by using software (FAMAS, Kyowa Interface Science Co., Ltd., Saitama, Japan) in the analyzer.

LPF and TOCN-LPFs were cut into a rectangular shape of 5 cm × 1 cm as a test specimen for tensile test. The specimen was fixed on a paper holder, and testing length of the resultant specimen was 3 cm. Then, the holder was set in a tensile test machine (Shimazu Autograph AGS-500D, Kyoto, Japan). The tensile speed was 10 mm/min. The stress was monitored by using a load cell during the tensile test.

Zero-span tensile test was conducted according to TAPPI T 231 cm-85. A LPF with a rectangular size of 25 mm × 20 mm was set on an attachment by metallic clamping jaws. The attachment was mounted in a Shimazu Autograph AGS-500D (Kyoto, Japan). The tensile speed was 10 mm/min.

For a tensile impact test, obtained films were cut into dumbbell-like specimen with a molding cutter in accordance with ISO 8256 type 4. The specimen was set on a tensile impact test machine (Yasuda Seiki Seisakujo, Hyogo, Japan). An absorption energy (E) at failure was calculated from the following equation according to ISO 8256.

$$E(\mathrm{J}) = \mathrm{WR}\left[\left(\cos\theta_\beta - \cos\theta_\alpha\right) - \left(\cos\theta_{\alpha'} - \cos\theta_\alpha\right)(\theta_\alpha + \theta_\beta)/(\theta_\alpha + \theta_{\alpha'})\right]$$

where W is hammer weight (30 gf in this measurement), R is a distance (m) between rotation center and gravity center of hammer, and angles of θ_α, $\theta_{\alpha'}$ and θ_β are a raising angle of hammer (150° in this experiment), a swing angle without specimen and a swing angle with specimen, respectively.

Friction coefficients were calculated, based on friction force measured on a Tribogear, HHS3000 (Shinto Science Co., Ltd, Tokyo, Japan). LPF and TOCN-LPFs were fixed on an aluminum plate with a double-sided adhesive tape. An aluminum ball as a load probe was placed on the films, and it moves reciprocally under a 150 gf load. The moving distance was 30 mm, moving rate was 2 mm/s, and reciprocation times was 10. Friction coefficients were calculated from the measured friction forces and the probe load.

Dynamic mechanical analysis (DMA) was carried out on a DMS6100/EXSTAR6000 (Seiko Instruments Inc., Chiba, Japan). A dried LPF with a rectangular size of 20 mm × 5 mm was set in the DMA machine, and DMA was measured in a range from − 90 to 300 °C at a strain frequency of 10 Hz and a heating rate of 2 °C/min.

Differential scanning calorimetry (DSC) was carried out under a nitrogen atmosphere on a DSC6200/EXSTAR6000 (Seiko Instruments Inc., Chiba, Japan). After 1st heating from r.t. to 150 °C in the heating rate of 20 °C/min, followed by rapid cooling with liquid nitrogen to − 100 °C, 2nd heating was conducted to 200 °C at the heating rate of 20 °C/min.

Images of LPF and TOCN-LPF

The films including acetone-washed films (mentioned later) prepared in this experiment were observed under an optical microscope (VK-9500 Violet Laser Color 3D profile microscope, Keyence Japan, Osaka, Japan), and a field emission-scanning electron microscope (FE-SEM, JSM-6301F, JOEL Ltd., Tokyo, Japan) at an accelerating voltage of 5 kV after gold sputtering.

EDLC assembly

Prior to the EDLC assembly, electrode was prepared by casting the slurry on an aluminum sheet, followed by drying and cutting into a circle shape (16 mm, in diameter). The slurry was comprised of commercially available activated carbon powder (AC powder, Wako Pure Chemical Industries, Co., Ltd., Tokyo, Japan), conductive carbon black (CB, Super P conductive, 99 + %, Alfa Aesar, Heysham, England) and sodium carboxymethyl cellulose (CMC) as a binder, at the weight ratio of 85:10:5 (You et al. 2015, 2016a, b).

The films prepared in this study and commercially available cellulosic separator (Mitsubishi Paper Mills Ltd., Tokyo, Japan) were cut out into a circle with 18 mm in diameter, followed by washing with acetone with shaking at room temperature for a day, where acetone was exchanged to new one 5 times. After air-drying, the resultant films were separately immersed in an electrolyte solution (1.0 M triethylmethylammonium tetrafluoroborate/propylene carbonate) together with electrodes for 3 h at r.t. During the immersing, the air in samples was removed in vacuo.

For an EDLC assembly, the separator material was sandwiched between a pair of electrode material, and the sandwich was set in the Two Electrodes Flat Cell

(2E-CELL-SUS, Eager Corporation, Osaka, Japan) in a glove box under a nitrogen atmosphere.

Electrochemical test

The electrochemical properties of the assembled EDLCs were evaluated by using an electrochemical workstation (Autolab PGSTAT302N FRA32M, Metrohm Autolab B.V., Tokyo, Japan). Cyclic voltammetry (CV) was performed with a potential window from 0 to 3 V at the scan rate of 0.05 V/s, and specific capacitance of single electrode was calculated from rectangular area in cyclic voltammogram according to the following equation (Davies and Yu 2011; Qu and Shi 1998).

$$C = \frac{4I}{m \cdot V/t}$$

where I is the current formed at the potential of 1.5 V, V/t is the potential scanning rate, and m refers to the total weight of the materials on two electrodes.

Galvanostatic charge/discharge (GCD) measurements were carried out at a current density of 2 A g^{-1} in the voltage range of 0–3 V. The specific capacitance of single electrode was calculated from the GCD curves according to the following equation (Davies and Yu 2011; Qu and Shi 1998).

$$C = \frac{4i}{m \cdot dV/dt}$$

where i is the applied current, and dV/dt is the slope obtained by fitting a straight line to the discharge curve over the range from 1.8 to 1.35 V (60–45% of Vmax, where Vmax is the maximum value of the operating potential window).

Electrochemical impedance spectroscopy was conducted at an amplitude voltage of 20 mV and a frequency range of 1–10^5 Hz. Intrinsic resistance and electron transfer resistance were calculated from Nyquist plot by using a software of Autolab NOVA1.8 (Metrohm Autolab B.V., Utrecht, Netherlands). The intrinsic resistance was an intercept value at the Z′ axis of semicircle or arc in Nyquist plot, and the charge transfer resistance was estimated from chord length of the arc (Wang et al. 2001; Liu et al. 2008; Mei et al. 2017).

Results and discussion

Preparation of TOCN-LPF

In the preparation of LPF from ternary components (PEG-L, MA, and PEG500k), chloroform was used as a solvent for all the components (Kubota et al. 2015). Water was used in the preparation of TOCN-LPF, because chloroform was not suitable to mix TOCN with PEG-L and PEG500k. As a result, the film was successfully prepared by hot-pressing.

Chemical characterization of LPF and TOCN-LPF

To confirm the formation of ester bond in polyester, two mode FT-IR measurements (transmission and ATR) were conducted for LPF and TOCN-LPF. Here, typical spectra for 1%-TOCN-LPF are shown in Fig. 1. As expected, a band of ester carbonyl group at around 1750 cm^{-1} was appeared in both spectrum. In addition, the figure tells us interesting information on the film structure. In the transmission mode, a band of hydroxy group around 3500 cm^{-1} was clearly observed for both LPF and TOCN-LPF spectra, while the band was observed only at low intensity in the spectra recorded in the ATR mode. It was assumed that the surface of the film had hydrophobic nature, and unreacted hydroxy groups remained inside the film. The hydrophobicity of the surface was probably due to effect of super hydrophobic Teflon mold used in the film preparation (Aryal et al. 2009; Tsunozaki and Kawaguchi 2009).

To confirm the surface hydrophobicity of LPF and 1%-TOCN-LPF in more detail, their contact angles for a water droplet were measured (Table 1). Both films showed high values of contact angle over 90°, until 1 min after the water drop. However, the contact angles decreased with prolonged time of measurement. This result suggested that water droplet gradually impregnated into the inside of films. Therefore, our assumption on the surface hydrophobicity and the inner hydrophilicity of the LPFs was confirmed by this contact angle measurement. Contact angles for TOCN-LPF at any moment were higher than those of LPF (Table 1). This phenomenon looks somewhat interesting, because TOCN is basically considered hydrophilic material. Here, it is noteworthy that TOCN has amphiphilic nature; hydrophobic and hydrophilic planes (Fujisawa et al. 2017; Tamura

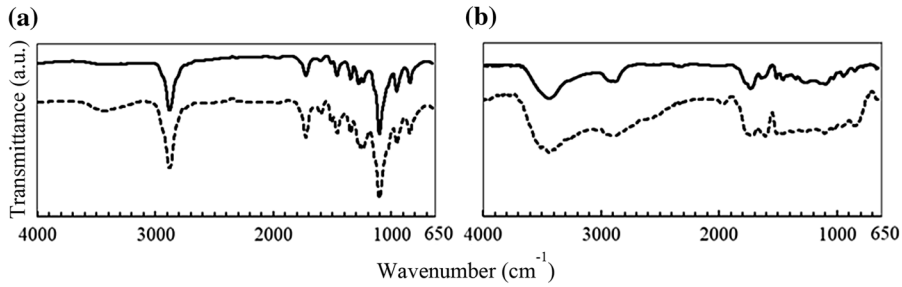

Fig. 1 **a** Transmission and **b** ATR FTIR spectra of LPF (dotted line) and 1%-TOCN LPF (solid line)

Table 1 Contact angles of water droplet against LPF and 1%-CNF LPF at each moment (°)

	0 s	30 s	1 min	5 min
LPF	106.3	99.4	93.8	49.9
1%-TOCN LPF	121.4	113.8	108.7	75.2

et al. 2018; Glasser et al. 2012; Yamane et al. 2006). It can thus be speculated that hydrophobic and hydrophilic planes of TOCN were oriented to the surface and the internal, respectively, during melt-polycondensation reaction.

Mechanical properties of LPF and TOCN-LPF

Figure 2 shows stress–strain curves of LPF and TOCN-LPFs with different TOCN contents in a general tensile test. Although LPF showed a large elongation ratio of about 90%, tensile strength at failure was less than 5 MPa. This revealed that LPF was flexible and brittle. By the addition of 1% TOCN, the tensile strength at failure was remarkably increased to about threefold that of LPF and more than 50% of the elongation ratio. As an evidence of flexibility, a paper aircraft could be folded from this 1%-TOCN-LPF as well as LPF (Supplemental Figure 1).

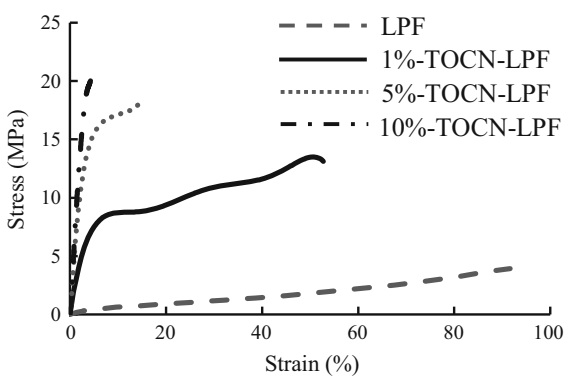

Fig. 2 Stress–strain curves of LPF and TOCN-LPFs

By further addition of TOCN (5% and 10%) to LPF, modulus of elasticity was markedly increased, but elongation ratio was much lower than that of 1% TOCN-LPF. Therefore, increased charge of TOCN rendered the film hard and brittle. Strain energy density, or so-called toughness, was calculated from the profiles of the stress–strain curves (Table 2). The 1%-TOCN-LPF indicated the highest value among the tested specimens, suggesting that the film had the ability to absorb strain energy.

A zero-span tensile test is generally used for clarification of a single fiber strength in the pulp and paper research (Hägglund et al. 2004). The tests for LPF and TOCN-LPFs were carried out to evaluate the effect of TOCN strength on the film strength (Supplemental Figure 2). The zero-span tensile strength at failure was also increased to about threefold that of LPF by 1% addition of TOCN, and other results demonstrated almost the same tendency as seen in general tensile tests. Therefore, it is considered that the fiber strength of TOCN added to the film affects positively general tensile strength of the film.

We also expected that TOCN would significantly improve resistance of LPF to physical impact. To confirm this expectation, tensile impact test was conducted for LPF and TOCN-LPFs. Table 2 shows no significant effect of TOCN; no clear increment of tensile impact strength was observed with an increase in TOCN amount.

Surface mechanical property of LPF and TOCN-LPFs

A tribology test under a 150 gf load was carried out to evaluate the effect of TOCN addition on the surface

Table 2 Mechanical properties of LPF and TOCN-LPFs

	Modulus of[1] elasticity (GPa)	Tensile[1] strength (Mpa)	Elongation[1] (%)	Strain energy[1] density (MJ m^{-3})	Tensile[2] impact strength (kJ m^{-2})
LPF	1.3×10^{-2}	3.9	91.9	1.70	992 ± 41
1%-TOCN LPF	0.3	13.2	52.9	5.45	1005 ± 9
5%-TOCN LPF	0.5	18.1	14.4	2.10	1083 ± 25
10%-TOCN LPF	0.7	20.2	4.5	0.55	1043 ± 3

[1]Results obtained from tensile test

[2]Results obtained from tensile impact test

mechanical property of the films (Fig. 3). Friction coefficients of LPF were gradually increased during measurement along with the repeated cycles. However, this phenomenon was remarkably suppressed by only 1% TOCN addition. Fluctuation of the friction coefficients was further suppressed by increasing addition of TOCN (3–10%), together with a decrease in the friction coefficients. Thus, it was confirmed that TOCN addition contributed to surface mechanical stability of LPF. Separator material always contacts with electrodes in EDLC cell, and the surface stability of LPF is important for maintaining electrochemical performance of EDLC when some external force is charged unexpectedly.

In this research, commercial cellulosic separator was used as a positive control material in the following section. Technical values of cellulosic separator for tensile strength and elongation were 24.4 MPa and 3.9%, respectively, which are much closer to those of 10%-TOCN-LPF (Table 2) than to those of 1%-TOCN-LPF. However, 1%-TOCN-LPF was used as the most suitable candidate for EDLC separator, based on its superior toughness and flexibility to other TOCN-LPFs. Flexibility of LPF as separator material was proved to be a key factor affecting electrochemical properties in our previous research (Kubota et al. 2015).

Thermal properties of LPF and TOCN-LPF

A wide temperature operation range is one of the EDLC advantages over secondary batteries (Parvini et al. 2015; Mejdoubi et al. 2018). Therefore, thermal property of LPF is also very important when it is used as a separator for EDLC. DMA and DSC measurement were conducted to monitor thermal deformation and viscoelasticity of LPF and 1%-TOCN-LPF. DMA and DSC profiles of LPF and TOCN-LPF are shown in Figs. 4 and 5, respectively. In the DMA profiles of LPF, E' and E'' were sharply decreased at around 50 °C, and then gradually decreased up to 150 °C. Afterwards, both moduli were sharply decreased again, and the film was collapsed at about 200 °C. In DSC profile of LPF, endothermic peak was observed

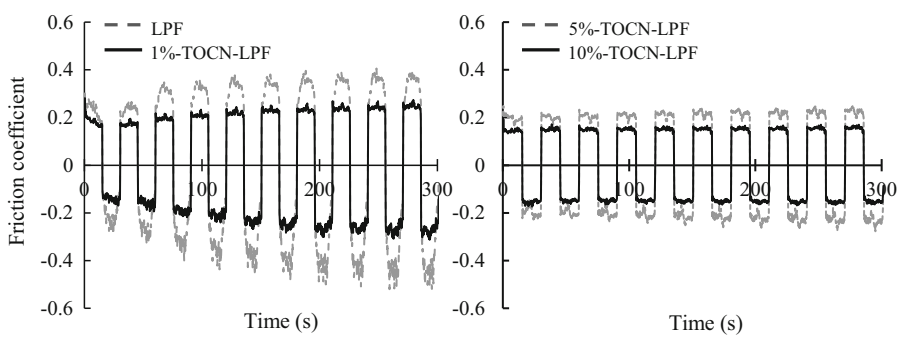

Fig. 3 Profiles of friction coefficient for LPF and TOCN-LPFs under a load of 150 gf in tribology test

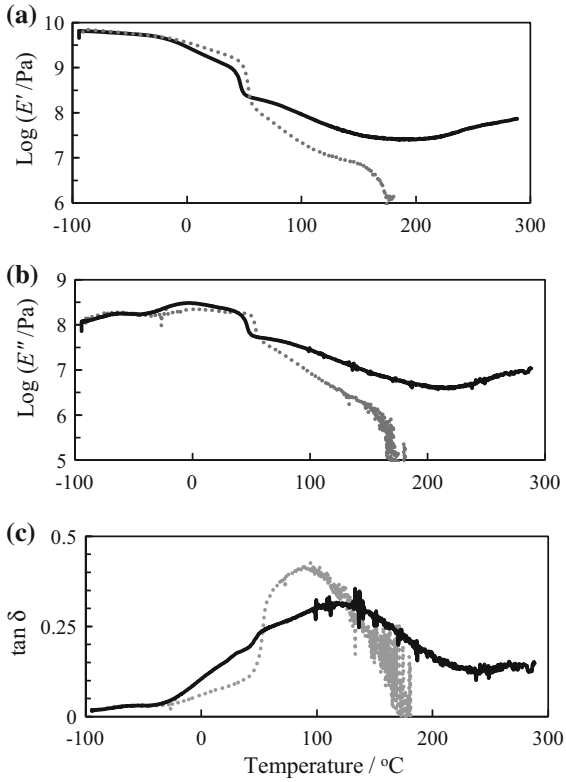

Fig. 4 Viscoelastic behavior of LPF (dotted line) and 1%-TOCN-LPF (solid line). **a** Storage modulus, **b** loss modulus, and **c** loss tangent

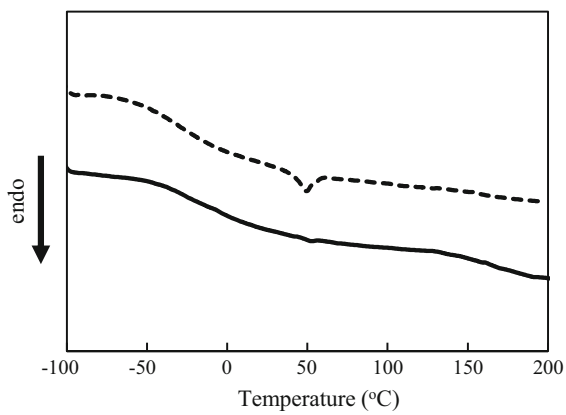

Fig. 5 DSC profiles of LPF (dotted line) and 1%-TOCN-LPF (solid line)

at 50 °C, which was close to the melting point of PEG with high molar mass. These results suggest that the clear reduction of E' and E'' at 50 °C was caused by the partial melting of PEG500k domain.

On the other hand, DMA profiles of TOCN-LPF revealed to suppress the reduction in both moduli at 50 °C, and also to suppress gradual reduction in the moduli over 50 °C. The DMA measurement could be done until 300 °C because no collapse was seen. In addition, TOCN-LPF showed a smaller endothermic peak of PEG500k at 55 °C. These results suggest that TOCN is a useful filler for LPF to suppress the thermal transformation and to maintain the viscoelastic moduli at a higher level. Such thermal stability of TOCN-LPF compared to LPF may enable EDLC operation at elevated temperature.

Electrochemical properties of TOCN-LPF

Electrochemical properties of EDLCs assembled with TOCN-LPF or cellulosic separator as a reference EDLC were evaluated from CV, GCD and EIS measurements (Sun et al. 2014). Prior to these measurements, TOCN-LPF was washed with acetone thoroughly, because unreacted components in the melt-polycondensation reaction might affect electrochemical performance. As a result of washing, 1%-TOCN-LPF with little pore was transformed into porous film, as shown in Fig. 6.

The cyclic voltammogram for EDLC with TOCN-LPF in Fig. 7 was found to be an almost perfect rectangular shape, indicating the formation of electric double layer in this EDLC. The specific capacitance was calculated from the rectangular area in cyclic voltammogram at the 5th scan, and was also obtained from GCD measurement at the 5th discharge step (Fig. 8). The specific capacitance values of EDLC with TOCN-LPF from CV and GCD was 92.0 F g^{-1} and 105.2 F g^{-1} respectively. These values were higher than those (83.2 F g^{-1} and 78.8 F g^{-1}, respectively) of the reference EDLC with cellulosic paper. In addition, the specific capacitance of EDLC with TOCN-LPF from CV (92.0 F g^{-1}) was much higher than that of EDLC with LPF measured previously (69.8 F g^{-1}, Kubota et al. 2015). Although a specific capacitance (F g^{-1}) is expressed based on a weight of electrode (Davies and Yu 2011; Qu and Shi 1998), electrolyte amount retained in EDLC system is not considered. Thereby, the electrolyte amount may also affect the capacitance. Based on this assumption, there are two reasons proposed for such a high specific capacitance of EDLC with TOCN-LPF. One is porous structure of acetone-washed film (Fig. 6), which

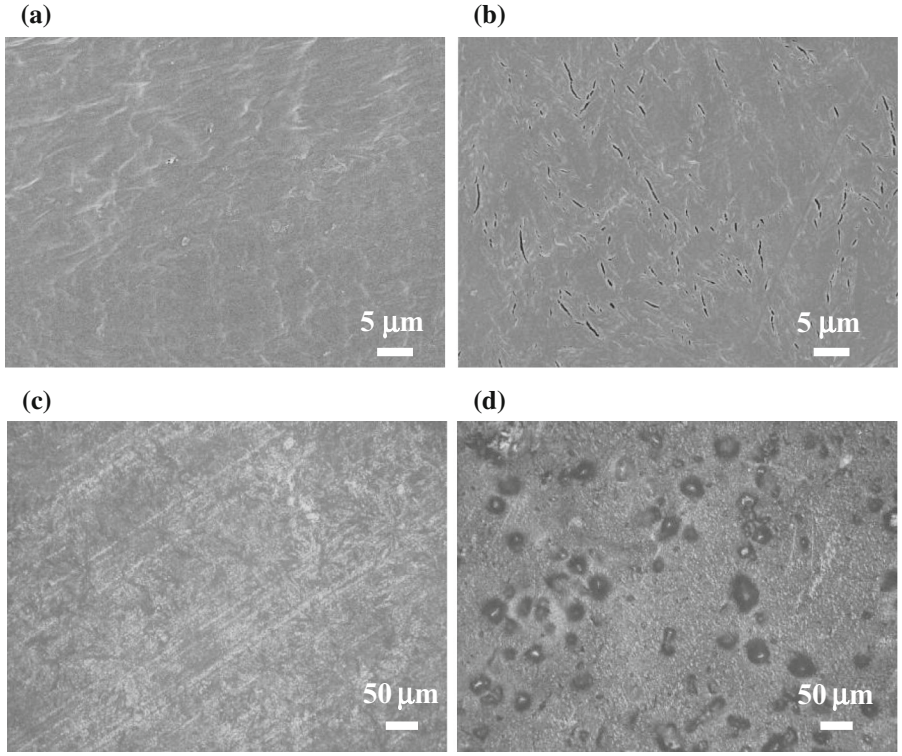

Fig. 6 SEM images of 1%-TOCN LPF **a** before and **b** after acetone-wash. Microscopic images of **c** 1%-TOCN LPF and **d** porous 1%-TOCN-LPF

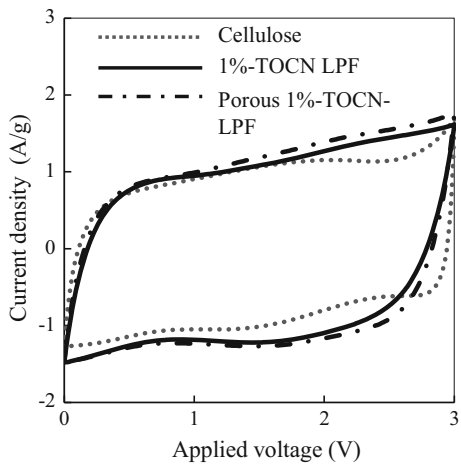

Fig. 7 Cyclic voltammograms of EDLCs assembled with different separator materials at a scan rate of 0.05 V s^{-1}

enables high permeability of electrolyte through the film and large retention of electrolyte because of its large surface area. The other one is the involvement of carboxy groups of TOCN in the electrolyte transportation and retention. However, the detailed mechanism has not yet been clearly elucidated.

Two kinds of resistances, intrinsic and charge transfer resistances, were determined from Nyquist plot obtained by EIS measurement. The plots are shown in Fig. 9. EDLC with TOCN-LPF showed much higher intrinsic resistance (26.1 Ω) and electron transfer resistance (8.1 Ω) than those (2.4 Ω and 1.7 Ω, respectively) of the reference EDLC with cellulosic paper. These high resistances must be attributed to the lack of electrolyte transportation through the film. To improve the electrolyte transportation, the conversion of TOCN-LPF into porous film was attempted by the addition of NaCl powder to the quaternary mixture (PEG-L, MA, PEG500k and TOCN), followed by washing out the NaCl powder with water. As a result, highly porous film was obtained, as shown in Fig. 6. As expected, the EDLC with this porous TOCN-LPF showed low intrinsic resistance (6.0 Ω) and electron transfer resistance (5.8 Ω). In addition, the specific capacitance (98.1 F g^{-1} from CV, and 111.1 F g^{-1} from GCD).

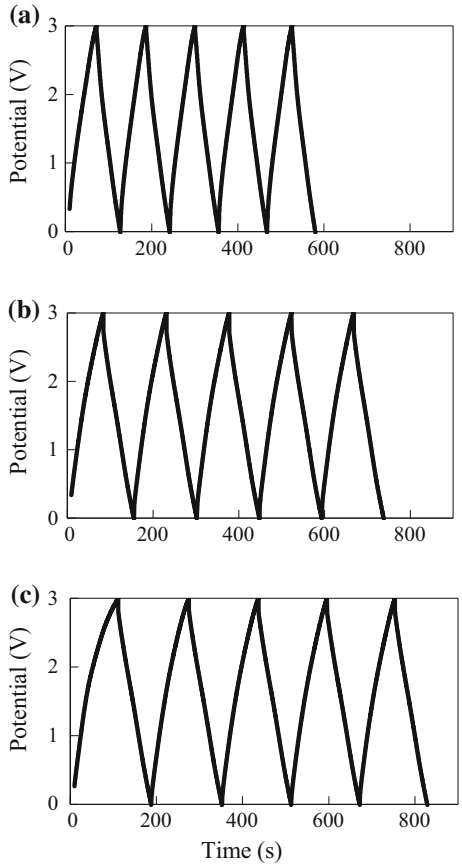

Fig. 8 GCD profiles of EDLCs with **a** cellulose, **b** TOCN-LPF and **c** porous TOCN-LPF under a current density of 2.0 A g^{-1}

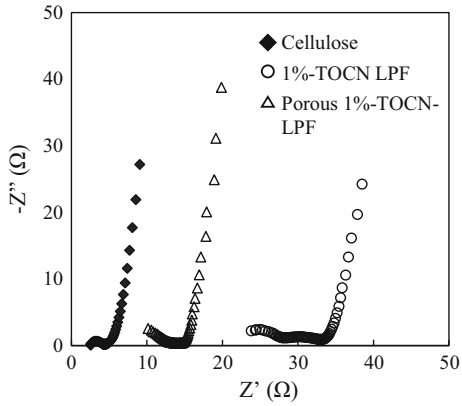

Fig. 9 Nyquist plots of EDLCs assembled with different separator materials

was also improved by this conversion. Thus, porous structure contributes to the high capacitances of both EDLCs with TOCN-LPF just after acetone-washing and with porous TOCN-LPF prepared by the NaCl addition.

Finally, GCD measurements for 100 cycles were conducted to evaluate cycle durability of EDLC with porous TOCN-LPF. The specific capacitance was gradually decreased with increasing the cycle numbers of charge and discharge process as well as the reference EDLC with cellulosic paper (Supplemental Figure 3). Both ratios of the capacitance at 100th scan to that at 1st scan were almost identical 71%. Therefore, the reduced performance of the capacitance was attributed to deterioration of EDLC electrode, but not to that of separator. Consequently, porous TOCN-LPF can be used as a separator suitable for EDLC.

Conclusion

Reinforcement of LPF with TOCN was attempted in this research. By the 1% addition of TOCN, tensile strength at failure was markedly increased to about threefold that of LPF strength with more than 50% of the elongation ratio maintained. As a result, its strain energy density was also threefold that of LPF. Fluctuation of friction coefficient of LPF was also suppressed by the TOCN addition, indicating improvement of stability of the film surface. Moreover, the TOCN addition imparted thermal stability to LPF. However, its addition did not affect the tensile impact strength.

EDLC with TOCN-LPF showed higher value of specific capacitance than that of aa reference EDLC with commercial cellulosic paper. Although intrinsic resistance and electron transfer resistance of the EDLC with TOCN-LPF was much higher than those of the reference EDLC, these resistances were improved by converting the TOCN-LPF to the porous film with NaCl before hot-pressing addition and NaCl removal after hot-pressing.

References

Arora P, Zhang Z (2004) Battery separators. Chem Rev 104:4419–4462. https://doi.org/10.1021/cr020738u

Aryal M, Trivedi K, Hu W (2009) Nano-confinement induced chain alignment in ordered P3HT nanostructures defined by nanoimprint lithography. ACS Nano 3:3085–3090. https://doi.org/10.1021/nn900831m

Calvo-Flores FG, Dobado JA (2010) Lignin as renewable raw material. Chemsuschem 3:1227–1235. https://doi.org/10.1002/cssc.201000157

Choi NS, Chen Z, Freunberger SA et al (2012) Challenges facing lithium batteries and electrical double-layer capacitors. Angew Chem Int Ed 51:9994–10024. https://doi.org/10.1002/anie.201201429

Davies A, Yu A (2011) Material advancements in supercapacitors: from activated carbon to carbon nanotube and graphene. Can J Chem Eng 89:1342–1357. https://doi.org/10.1002/cjce.20586

Fujisawa S, Togawa E, Kuroda K (2017) Facile route to transparent, strong, and thermally stable nanocellulose/polymer nanocomposites from an aqueous pickering emulsion. Biomacromol 18:266–271. https://doi.org/10.1021/acs.biomac.6b01615

Gillet S, Aguedo M, Petitjean L et al (2017) Lignin transformations for high value applications: towards targeted modifications using green chemistry. Green Chem 19:4200–4233. https://doi.org/10.1039/c7gc01479a

Glasser WG, Atalla RH, Blackwell J et al (2012) About the structure of cellulose: debating the Lindman hypothesis. Cellulose 19:589–598. https://doi.org/10.1007/s10570-012-9691-7

Gogotsi Y, Simon P (2011) True performance metrics in electrochemical energy storage. Science 334:917–918. https://doi.org/10.1126/science.1213003

Hägglund R, Gradin PA, Tarakameh D (2004) Some aspects on the zero-span tensile test. Exp Mech 44:365–374. https://doi.org/10.1177/0014485104046085

He F, Zhao D (2007) Manipulating the size and dispersibility of zerovalent iron nanoparticles by use of carboxymethyl cellulose stabilizers. Environ Sci Technol 41:6216–6221. https://doi.org/10.1021/es0705543

Isogai A, Saito T, Fukuzumi H (2011) TEMPO-oxidized cellulose nanofibers. Nanoscale 3:71–85. https://doi.org/10.1039/C0NR00583E

Kaitsuka Y, Hayashi N, Shimokawa T et al (2016) Synthesis of polyaniline (PANI) in nano-reaction field of cellulose nanofiber (CNF), and carbonization. Polymers 8:40–51. https://doi.org/10.3390/polym8020040

Kose R, Mitani I, Kasai W et al (2011) "Nanocellulose" as a single nanofiber prepared from pellicle secreted by gluconacetobacter xylinus using aqueous counter collision. Biomacromol 12:716–720. https://doi.org/10.1021/bm1013469

Koumba-Yoya G, Stevanovic T (2017) Study of organosolv lignins as adhesives in wood panel production. Polymers 9:46–58. https://doi.org/10.3390/polym9020046

Kubota A, Isozaki T, Yamada T et al (2015) Development of new polyester film from ceder-organosolv lignin and its application for a separator in electric double-layer capacitor. In: Proceedings of the 18th international symposium on wood, fibre and pulping chemistry, Sept 9–11, Vienna, Austria (Oral Presentation), pp 167–168

Lee S, Pan H, Hse CY et al (2014) Characteristics of regenerated nanocellulosic fibers from cellulose dissolution in aqueous solutions for wood fiber/polypropylene composites. J Thermoplast Compos Mater 27:558–570. https://doi.org/10.1177/0892705713484739

Li J, Lewis RB, Dahn JR (2007) Sodium carboxymethyl cellulose a potential binder for Si negative electrodes for Li-ion batteries. Electrochem Solid State Lett 10:A17–A20. https://doi.org/10.1149/1.2398725

Lin J, Kubo S, Yamada T et al (2012) Chemical thermostabilization for the preparation. BioResources 7:5634–5646. https://doi.org/10.15376/biores.7.4.5634-5646

Liu C-L, Dong W, Cao G et al (2008) Capacitance limits of activated carbon fiber electrodes in aqueous electrolyte. J Electrochem Soc 155:F1–F7. https://doi.org/10.1149/1.2799683

Mei BA, Munteshari O, Lau J et al (2017) Physical interpretations of Nyquist plots for EDLC electrodes and devices. J Phys Chem C 122:194–206. https://doi.org/10.1021/acs.jpcc.7b10582

Mejdoubi AE, Chaoui H, Sabor J, Gualous H (2018) Remaining useful life prognosis of supercapacitors under temperature and voltage aging conditions. IEEE Trans Ind Electron 65:4357–4367. https://doi.org/10.1109/TIE.2017.2767550

Nihat SC, Nilgül O (2002) Use of organosolv lignin in phenol formaldehyde resins for particleboard production II. Particleboard production and properties. Int J Adhes Adhes 22:477–480. https://doi.org/10.1016/S0143-7496(02)00058-1

Noorden ZA, Sugawara S, Matsumoto S (2014) Noncorrosive separator materials for electric double layer capacitor. IEEJ Trans Electr Electron Eng 9:235–240. https://doi.org/10.1002/tee.21961

Okita Y, Saito T, Isogai A (2010) Entire surface oxidation of various cellulose microfibrils by TEMPO mediated oxidation. Biomacromol 11:1696–1700. https://doi.org/10.1021/bm100214b

Parvini Y, Siegel J, Stefanopoulou A, Vahidi A (2015) Supercapacitor electrical and thermal modeling, identification, and validation for a wide range of temperature and power applications. IEEE Trans Ind Electron 63:1574–1585. https://doi.org/10.1109/TIE.2015.2494868

Qu D, Shi H (1998) Studies of activated carbons used in double-layer capacitors. J Power Sources 74:99–107. https://doi.org/10.1016/S0378-7753(98)00038-X

Saito T, Hirota M, Tamura N et al (2009) Individualization of nano-sized plant cellulose fibrils achieved by direct surface carboxylation using TEMPO catalyst under neutral conditions. Biomacromol 10:1992–1996. https://doi.org/10.1021/bm900414t

Sharma P, Bhatti TS (2010) A review on electrochemical double-layer capacitors. Energy Convers Manag 51:2901–2912. https://doi.org/10.1016/j.enconman.2010.06.031

Sugimura K, Teramoto Y, Nishio Y (2015) Insight into miscibility behaviour of cellulose ester blends with N-vinyl pyrrolidone copolymers in terms of viscometric interaction parameters. Cellulose 22:2349–2363. https://doi.org/10.1007/s10570-015-0660-9

Sun XZ, Zhang X, Huang B, Ma YW (2014) Effects of separator on the electrochemical performance of electrical double-layer capacitor and hybrid battery-supercapacitor. Wuli Huaxue Xuebao/Acta Phys Chim Sin 30:485–491. https://doi.org/10.3866/PKU.WHXB201401131

Szubzda B, Szmaja A, Ozimek M, Mazurkiewicz S (2014) Polymer membranes as separators for supercapacitors.

Appl Phys A Mater Sci Process 117:1801–1809. https://doi.org/10.1007/s00339-014-8674-y

Tamura Y, Kanomata K, Kitaoka T (2018) Interfacial hydrolysis of acetals on protonated tempo-oxidized cellulose nanofibers. Sci Rep 8:6–10. https://doi.org/10.1038/s41598-018-23381-8

Tõnurist K, Thomberg T, Jänes A et al (2012) Specific performance of electrical double layer capacitors based on different separator materials in room temperature ionic liquid. Electrochem Commun 22:77–80. https://doi.org/10.1016/j.elecom.2012.05.029

Tsunozaki K, Kawaguchi Y (2009) Preparation methods and characteristics of fluorinated polymers for mold replication. Microelectron Eng 86:694–696. https://doi.org/10.1016/j.mee.2008.11.002

Wang C, Appleby AJ, Little FE (2001) Electrochemical impedance study of initial lithium ion intercalation into graphite powders. Electrochim Acta 46:1793–1813. https://doi.org/10.1016/S0013-4686(00)00782-9

Wu W, Dutta T, Varman AM et al (2017) Lignin valorization: two hybrid biochemical routes for the conversion of polymeric lignin into value-added chemicals. Sci Rep 7:1–13. https://doi.org/10.1038/s41598-017-07895-1

Yamane C, Aoyagi T, Ago M et al (2006) Two different surface properties of regenerated cellulose due to structural anisotropy. Polym J 38:819–826. https://doi.org/10.1295/polymj.PJ2005187

Yano H, Sugiyama J, Nakagaito AN et al (2005) Optically transparent composites reinforced with networks of bacterial nanofibers. Adv Mater 17:153–155. https://doi.org/10.1002/adma.200400597

You X, Koda K, Yamada T, Uraki Y (2015) Preparation of electrode for electric double layer capacitor from electrospun lignin fibers. Holzforschung 69:1097–1106. https://doi.org/10.1515/hf-2014-0262

You X, Duan J, Koda K et al (2016a) Preparation of electric double layer capacitors (EDLCs) from two types of electrospun lignin fibers. Holzforschung 70:661–671. https://doi.org/10.1515/hf-2015-0175

You X, Koda K, Yamada T, Uraki Y (2016b) Preparation of high-performance internal tandem electric double-layer capacitors (IT-EDLCs) from melt-spun lignin fibers. J Wood Chem Technol 36:418–431. https://doi.org/10.1080/02773813.2016.1212893